Progress in Fractional Differentiation and Applications
An International Journal

http://dx.doi.org/10.18576/pfda/120101

A Nonstandard Two-Step Lagrange Interpolation Method for Fractional-Order Influenza Model: Comparative Study with Real Data

Nasser Hassan Sweilam[1,*], *Nourhan Hamdy*[2], *Ehab A. El-Sayed*[2] *and Tarek Emam*[3]

[1] Mathematics Department, Faculty of Science, Cairo University, Giza, Egypt
[2] Engineering Sciences and Mathematics Department, Faculty of Petroleum and Mining Engineering, Suez University, Suez, Egypt
[3] Department of Mathematics, Faculty of Science, Suez University, Suez, Egypt

Received: 2 Apr. 2025, Revised: 18 Jul. 2025, Accepted: 20 Aug. 2025
Published online: 1 Jan. 2026

Abstract: This paper's major goal is to introduce novel computational studies of the fractional-order influenza mathematical model by utilizing three definitions for the fractional-order derivatives. For these models, the fractional derivatives were defined using the Caputo, Caputo-Fabrizio, and Atangana-Baleanu-Caputo definitions. Using the nonstandard two-step Lagrange interpolation approach, the fractional-order models become fitted. There are comparative analyses and numerical simulations provided to demonstrate and comprehend our findings. Moreover, comparative studies between the proposed definitions and the Kingdom of Saudi Arabia's data on influenza cases per week demonstrate how well the suggested models capture the dynamics of disease.

Keywords: Influenza Mathematical model; fractional-order derivatives; Numerical analysis; The nonstandard two-step Lagrange interpolation method.

1 Introduction

Influenza viruses are categorized into various classifications, with influenza A and B being the most important factors in the cause of respiratory infections [1,2]. Influenza A, which causes pandemics and seasonal epidemics, is the most severe and pervasive form. It is further divided into subgroups according to its surface proteins [3,4]. In contrast, influenza B primarily affects humans and is less severe, not being classified into sub-types. Seasonal influenza, which occurs annually throughout the winter, is brought on by influenza A and B, leading to significant public health concerns and necessitating annual vaccination campaigns. Furthermore, influenza C poses less of a threat to public health overall and is not linked to pandemics or seasonal outbreaks, despite the fact that it can cause mild respiratory infections [5,6]. Understanding these distinctions is crucial for effective prevention and response strategies against influenza-related illnesses. Since models are essential for explaining events that occur globally in numerous domains, including technology, engineering, and science, researchers require assistance in creating them [7,8,9,10,11,12,13,14].

After centuries of modest progress, fractional calculus has seen a rise in applications in recent decades. There are examples in numerous scientific domains, including epidemiology, biology, and engineering [9,15,16,17,18]. Typically, models of fractional-order differential equations (FODEs) appear to be more in line with actual phenomena than models of integer order [19,20,21,22]. The ability to describe the memory and inherited characteristics present in different materials and processes seen in the majority of biological systems is made possible by fractional derivatives and integrals [23,24]. More recently, a modified Caputo fractional derivative was developed in the meaning of the Atangana-Baleanu-Caputo sense (ABC) by presenting a numerical approach in which the fundamental theorem of fractional calculus and the two-step Lagrange polynomial are combined [25]. These novel derivative types have been utilized in the simulation of practical applications across diverse domains [26,27].

Influenza mathematical models have been employed to comprehend and forecast the virus's spread, assess the influence of controlling measures, and guide public health efforts. The primary contribution of this paper is presenting

* Corresponding author e-mail: nsweilam@sci.cu.edu.eg

the fractional models' effectiveness in relation to influenza dynamics, particularly Caputo (C), Caputo-Fabrizio (CF), and Atangana–Baleanu-Caputo (ABC) definitions [28]. The nonstandard two-step Lagrange interpolation method (NS2LIM) is the numerical methodology used [29]. There are numerical simulations provided. This study stands out for its thorough evaluation of the fractional-order models effectiveness; especially the ABC model is the better option for epidemiological modeling compared to the other two models. The NS2LIM with the ABC operator is the better option for epidemiological modeling compared to the other two operators. Additionally, the ABC operator has shown an improvement in their ability to accurately reflect the accurate data, which is what makes this work new.

This manuscript is structured in the following manner: An overview of the first ideas utilized during our research is given at the start of section 2. A demonstration is given of the model's transformation according to of fractional derivatives in Section 3. The influenza model's numerical approaches are given in section 4. In Section 5, there is a description of simulations and numerical studies. Section 6 concludes with a discussion of the conclusions.

2 Preliminaries

Within this part, We will review some fundamental definitions of fractional calculus that will be utilized in the future sections.

The derivative of Liouville-Caputo fractional-order (α) that is outlined in the definition [29,30]

$$ {}_0^C D_t^\alpha z(t) = \frac{1}{\Gamma(1-\alpha)} \int_0^t (t-\vartheta)^{-\alpha} z'(\vartheta) d\vartheta \quad , 0<\alpha \leq 1. \tag{1} $$

The derivative of CF fractional-order α in Liouville–Caputo sense that is outlined in the definition [29]

$$ {}_0^{CFC} D_t^\alpha z(t) = M(\alpha) \frac{(2-\alpha)}{2(1-\alpha)} \int_0^t exp\Big(\frac{-\alpha(t-\vartheta)}{1-\alpha}\Big) z'(\vartheta) d\vartheta \quad , 0<\alpha \leq 1, \tag{2} $$

where the normalizing function is $M(\alpha) = \frac{2}{2-\alpha}$. The derivative of AB fractional-order α in Liouville–Caputo sense that is outlined in the definition [31]

$$ {}_0^{ABC} D_t^\alpha z(t) = B(\alpha) \frac{1}{1-\alpha} \int_0^t E_\alpha\Big(\frac{-\alpha(t-\vartheta)^\alpha}{1-\alpha}\Big) z'(\vartheta) d\vartheta \quad , 0<\alpha \leq 1, \tag{3} $$

where the normalizing function is $B(\alpha) = 1 + \frac{\alpha}{\Gamma(\alpha)} - \alpha$.

3 The Influenza model

The SEIR model is used to represent influenza transmission dynamics by split the community up into four distinct groups: S susceptible, E exposed, I infectious, and R recovered. As a result,

$$ N(t) = S(t) + E(t) + I(t) + R(t), $$

at any given time t. Where, N is the population's overall size.
The following system (4) of nonlinear ordinary differential equations formally represents the epidemiological mathematical model of the SEIR influenza virus:

$$ \begin{aligned} \frac{dS}{dt} &= \eta_0 N - \eta_1 S - \eta_2 \frac{IS}{N}, \\ \frac{dE}{dt} &= \eta_2 \frac{IS}{N} - (\eta_1 + \eta_3) E, \\ \frac{dI}{dt} &= \eta_3 E - (\eta_1 + \eta_4) I, \\ \frac{dR}{dt} &= \eta_4 I - \eta_1 R. \end{aligned} \tag{4} $$

The model parameters are fully explained in tables 1,2, for the initial conditions of $R_0 \geq 0, I_0 \geq 0, E_0 \geq 0$, and $S_0 \geq 0$. For more details see [28].

Table 1: Explanation of the SEIR model's variables.

Variables	Explanation
S	Category that is susceptible
E	Category that is exposed
I	Category that is infected
R	Category that is recovered

Table 2: description of the parameters of the SEIR model.

Parameter	Description	Value
η_0	The natural rate of birth	0.01
η_1	The natural rate of death	0.09
η_2	The rate of transmission	0.98
η_3	The rate of incubation	0.78
η_4	The rate of recovery	0.62

Systems (4) have the following basic reproduction number [28]:

$$R_0 = \frac{\eta_0\eta_2\eta_3}{\eta_1(\eta_1+\eta_3)(\eta_1+\eta_4)},$$

If the influenza model's basic reproduction number is $R_0 > 1$, it has the possibility of spreading throughout a population. On the other hand, the infection will be eliminated if $R_0 < 1$. $E^* = (S^*, E^*, I^*, R^*)$, is the system's endemic equilibrium (4), with S^*, E^*, I^*, R^* being as follows:

$$S^* = \frac{(\eta_1+\eta_3)(\eta_1+\eta_4)}{\eta_2\eta_3}N,$$
$$E^* = \frac{\eta_4}{\eta_1}I,$$
$$I^* = \frac{(\eta_2\eta_3-(\eta_1+\eta_4)(\eta_1+\eta_3))\eta_1}{(\eta_1\eta_3-\eta_1(\eta_4+\eta_1)-\eta_4\eta_3)\eta_2}N,$$
$$R^* = \frac{\eta_4+\eta_1}{\eta_3}I.$$

4 NS2LIM for solving SEIR model

Here, the fractional influenza model of (4) is shown. The characterization of fractional models, corresponding to systems dependent on memory, requires the use of various methodologies. A flexible approach is possible through the use of the two-step Lagrange interpolation method that is especially used in computational and numerical analytic applications. This can increase accuracy in large-scale problems and greatly reduced computational time [32,33]. This numerical method for three fractional differential operators will be reviewed below.

4.1 *The model problem using Caputo derivative*

The influenza model under Caputo operator.

$$\begin{aligned} {}_0^C D_t^\alpha S(t) &= \eta_0 N - \eta_1 S - \eta_2 \frac{IS}{N}, \\ {}_0^C D_t^\alpha E(t) &= \eta_2 \frac{IS}{N} - (\eta_1 + \eta_3) E, \\ {}_0^C D_t^\alpha I(t) &= \eta_3 E - (\eta_1 + \eta_4) I, \\ {}_0^C D_t^\alpha R(t) &= \eta_4 I - \eta_1 R. \end{aligned} \tag{5}$$

For simplicity consider the model as follows:

$$\begin{aligned} {}_0^C D_t^\alpha z(t) &= Q(t, z(t)) \quad ,0<t \leq T \quad ,0<\alpha \leq 1, \\ z(0) &= z_0. \end{aligned} \tag{6}$$

The fundamental theorem of fractional calculus is applied to obtain,

$$z(t) = z(0) + \frac{1}{\Gamma(\alpha)} \int_0^t Q(\vartheta, z(\vartheta))(t-\vartheta)^{\alpha-1} d\vartheta, \tag{7}$$

For t_{k+1}, we get

$$z(t_{k+1}) = z(0) + \frac{1}{\Gamma(\alpha)} \sum_{v=0}^{k} \int_{t_v}^{t_{v+1}} Q(\vartheta, z(\vartheta))(t_{k+1}-\vartheta)^{\alpha-1} d\vartheta, \tag{8}$$

Here is the two-step Lagrange interpolation:

$$P_n \simeq \frac{Q(t_v, z_v)}{h}(\vartheta - t_{v-1}) - \frac{Q(t_{v-1}, z_{v-1})}{h}(\vartheta - t_v), \tag{9}$$

Replace equation (9) in (8) and performing the same steps in [29], we get

$$\begin{aligned} z(t_{k+1}) = z(0) + \frac{1}{\Gamma(\alpha)} \sum_{v=0}^{k} \Bigg(& \frac{h^\alpha Q(t_v, z_v)}{\alpha(\alpha+1)} \Big((2+\alpha+k-v)(k+1-v)^\alpha - (2+2\alpha+k-v)(k-v)^\alpha \Big) \\ & - \frac{h^\alpha Q(t_{v-1}, z_{v-1})}{\alpha(\alpha+1)} \Big((k+1-v)^{\alpha+1} - (1+\alpha+k-v)(k-v)^\alpha \Big) \Bigg). \end{aligned} \tag{10}$$

In order to achieve great stability [34], we make one simple modification in (10). This change involves substituting $\phi(h)$ for the step size h so that $\phi(h) = h + O(h^2), 0 < \phi(h) \leq 1$. Refer to [35,36,37,38,39] for additional information about NSFDM. As follows, the NS2LIM is presented:

$$\begin{aligned} z(t_{k+1}) = z(0) + \frac{1}{\Gamma(\alpha)} \sum_{v=0}^{k} \Bigg(& \frac{\phi(h)^\alpha Q(t_v, z_v)}{\alpha(\alpha+1)} \Big((2+\alpha+k-v)(k+1-v)^\alpha - (2+2\alpha+k-v)(k-v)^\alpha \Big) \\ & - \frac{\phi(h)^\alpha Q(t_{v-1}, z_{v-1})}{\alpha(\alpha+1)} \Big((k+1-v)^{\alpha+1} - (1+\alpha+k-v)(k-v)^\alpha \Big) \Bigg). \end{aligned} \tag{11}$$

The parameters and the initial values will be described within the system building phase as follows:

Algorithm 1: System building phase

1- Define the parameters η_i for each $i = 0, 1, ..., 4$.
2- Within a time period $0<t \leq T$ calculate $n = \frac{T-0}{h}$.
3- Initialize the values of the variables.

After building the system, proceed the NS2LIM for the Caputo definition.

Algorithm 2: NS2LIM under Caputo definition

For every step calculate the values of the system:

$$
\begin{aligned}
S(t_{k+1}) &= S(0)+\frac{1}{\Gamma(\alpha)}\sum_{v=0}^{k}\left(\frac{\phi(h)^{\alpha}Q(t_v,S_v)}{\alpha(\alpha+1)}\left((2+\alpha+k-v)(k+1-v)^{\alpha}-(2+2\alpha+k-v)(k-v)^{\alpha}\right)\right.\\
&\left.-\frac{\phi(h)^{\alpha}Q(t_{v-1},S_{v-1})}{\alpha(\alpha+1)}\left((k+1-v)^{\alpha+1}-(1+\alpha+k-v)(k-v)^{\alpha}\right)\right).\\
E(t_{k+1}) &= E(0)+\frac{1}{\Gamma(\alpha)}\sum_{v=0}^{k}\left(\frac{\phi(h)^{\alpha}Q(t_v,E_v)}{\alpha(\alpha+1)}\left((2+\alpha+k-v)(k+1-v)^{\alpha}-(2+2\alpha+k-v)(k-v)^{\alpha}\right)\right.\\
&\left.-\frac{\phi(h)^{\alpha}Q(t_{v-1},E_{v-1})}{\alpha(\alpha+1)}\left((k+1-v)^{\alpha+1}-(1+\alpha+k-v)(k-v)^{\alpha}\right)\right).\\
I(t_{k+1}) &= I(0)+\frac{1}{\Gamma(\alpha)}\sum_{v=0}^{k}\left(\frac{\phi(h)^{\alpha}Q(t_v,I_v)}{\alpha(\alpha+1)}\left((2+\alpha+k-v)(k+1-v)^{\alpha}-(2+2\alpha+k-v)(k-v)^{\alpha}\right)\right.\\
&\left.-\frac{\phi(h)^{\alpha}Q(t_{v-1},I_{v-1})}{\alpha(\alpha+1)}\left((k+1-v)^{\alpha+1}-(1+\alpha+k-v)(k-v)^{\alpha}\right)\right).\\
R(t_{k+1}) &= R(0)+\frac{1}{\Gamma(\alpha)}\sum_{v=0}^{k}\left(\frac{\phi(h)^{\alpha}Q(t_v,R_v)}{\alpha(\alpha+1)}\left((2+\alpha+k-v)(k+1-v)^{\alpha}-(2+2\alpha+k-v)(k-v)^{\alpha}\right)\right.\\
&\left.-\frac{\phi(h)^{\alpha}Q(t_{v-1},R_{v-1})}{\alpha(\alpha+1)}\left((k+1-v)^{\alpha+1}-(1+\alpha+k-v)(k-v)^{\alpha}\right)\right).
\end{aligned}
$$

End for

4.2 *The model problem using Caputo–Fabrizio derivative*

The influenza model under CFC operator.

$$
\begin{aligned}
{}_0^{CFC}D_t^{\alpha}S(t) &= \eta_0 N-\eta_1 S-\eta_2\frac{IS}{N},\\
{}_0^{CFC}D_t^{\alpha}E(t) &= \eta_2\frac{IS}{N}-(\eta_1+\eta_3)E,\\
{}_0^{CFC}D_t^{\alpha}I(t) &= \eta_3 E-(\eta_1+\eta_4)I,\\
{}_0^{CFC}D_t^{\alpha}R(t) &= \eta_4 I-\eta_1 R.
\end{aligned}
\tag{12}
$$

For simplicity consider the model as follows:

$$
\begin{aligned}
{}_0^{CFC}D_t^{\alpha}z(t) &= Q(t,z(t)) \quad ,0<t\le T,0<\alpha\le 1,\\
z(0) &= z_0.
\end{aligned}
\tag{13}
$$

The fundamental theorem of fractional calculus is applied to obtain,

$$
z(t)=z(0)+\frac{1-\alpha}{M(\alpha)}Q(t,z(t))+\frac{\alpha}{M(\alpha)}\int_0^t Q(\vartheta,z(\vartheta))d\vartheta,
\tag{14}
$$

where the normalizing function is $M(\alpha)=\frac{2}{2-\alpha}$. such that $M(0)=M(1)=1$. We obtained

$$
z(t_{k+1})=z(0)+\frac{(2-\alpha)(1-\alpha)}{2}Q(t_k,z(t_k))+\frac{\alpha(2-\alpha)}{2}\int_0^{t_{k+1}}Q(t,z(t))dt,
\tag{15}
$$

and

$$
z(t_k)=z(0)+\frac{(2-\alpha)(1-\alpha)}{2}Q(t_{k-1},z(t_{k-1}))+\frac{\alpha(2-\alpha)}{2}\int_0^{t_k}Q(t,z(t))dt,
\tag{16}
$$

Applying (16) in (15) see [26], we get

$$\begin{aligned} z(t_{k+1}) = z(k) + \left(\frac{(2-\alpha)(1-\alpha)}{2} + \frac{3h}{4}\alpha(2-\alpha)\right)Q(t_k, z(t_k)) \\ - \left(\frac{(2-\alpha)(1-\alpha)}{2} + \frac{h}{4}\alpha(2-\alpha)\right)Q(t_{k-1}, z(t_{k-1})). \end{aligned} \tag{17}$$

As follows, the NS2LIM is presented.

$$\begin{aligned} z(t_{k+1}) = z(k) + \left(\frac{(2-\alpha)(1-\alpha)}{2} + \frac{3\phi(h)}{4}\alpha(2-\alpha)\right)Q(t_k, z(t_k)) \\ - \left(\frac{(2-\alpha)(1-\alpha)}{2} + \frac{\phi(h)}{4}\alpha(2-\alpha)\right)Q(t_{k-1}, z(t_{k-1})). \end{aligned} \tag{18}$$

The following algorithm describes the simple calculation of the model under the CFC operator using the NS2LIM approach:

Algorithm 3: The CFC model with NS2LIM approach

For every $k = 0ton$ calculate the values of:

$$\begin{aligned} S(t_{k+1}) &= S(k) + \left(\frac{(2-\alpha)(1-\alpha)}{2} + \frac{3\phi(h)}{4}\alpha(2-\alpha)\right)Q(t_k, S(t_k)) \\ &\quad - \left(\frac{(2-\alpha)(1-\alpha)}{2} + \frac{\phi(h)}{4}\alpha(2-\alpha)\right)Q(t_{k-1}, S(t_{k-1})), \\ E(t_{k+1}) &= E(k) + \left(\frac{(2-\alpha)(1-\alpha)}{2} + \frac{3\phi(h)}{4}\alpha(2-\alpha)\right)Q(t_k, E(t_k)) \\ &\quad - \left(\frac{(2-\alpha)(1-\alpha)}{2} + \frac{\phi(h)}{4}\alpha(2-\alpha)\right)Q(t_{k-1}, E(t_{k-1})), \\ I(t_{k+1}) &= z(k) + \left(\frac{(2-\alpha)(1-\alpha)}{2} + \frac{3\phi(h)}{4}\alpha(2-\alpha)\right)Q(t_k, I(t_k)) \\ &\quad - \left(\frac{(2-\alpha)(1-\alpha)}{2} + \frac{\phi(h)}{4}\alpha(2-\alpha)\right)Q(t_{k-1}, I(t_{k-1})), \\ R(t_{k+1}) &= R(k) + \left(\frac{(2-\alpha)(1-\alpha)}{2} + \frac{3\phi(h)}{4}\alpha(2-\alpha)\right)Q(t_k, R(t_k)) \\ &\quad - \left(\frac{(2-\alpha)(1-\alpha)}{2} + \frac{\phi(h)}{4}\alpha(2-\alpha)\right)Q(t_{k-1}, R(t_{k-1})). \end{aligned}$$

End for

4.3 *The model problem using Atangana–Baleanu–Caputo derivative*

The influenza model under ABC operator.

$$\begin{aligned} {}^{ABC}_{0}D^{\alpha}_{t} S(t) &= \eta_0 N - \eta_1 S - \eta_2 \frac{IS}{N}, \\ {}^{ABC}_{0}D^{\alpha}_{t} E(t) &= \eta_2 \frac{IS}{N} - (\eta_1 + \eta_3)E, \\ {}^{ABC}_{0}D^{\alpha}_{t} I(t) &= \eta_3 E - (\eta_1 + \eta_4)I, \\ {}^{ABC}_{0}D^{\alpha}_{t} R(t) &= \eta_4 I - \eta_1 R. \end{aligned} \tag{19}$$

We have,

$$\begin{aligned} {}^{ABC}_{0}D^{\alpha}_{t} z(t) &= Q(t, z(t)) \quad , 0<t \le T, 0<\alpha \le 1, \\ z(0) &= z_0. \end{aligned} \tag{20}$$

The fundamental theorem of fractional calculus is applied to obtain,

$$z(t)=z(0)+\frac{1-\alpha}{B(\alpha)}Q(t,z(t))+\frac{\alpha}{\Gamma(\alpha)B(\alpha)}\int_0^t Q(\vartheta,z(\vartheta))(t-\vartheta)^{\alpha-1}d\vartheta, \tag{21}$$

Where the normalizing function is $B(\alpha)=1+\frac{\alpha}{\Gamma(\alpha)}-\alpha$.

At t_{k+1}, we get

$$\begin{aligned} z(t_{k+1}) &= z(0)+\frac{\Gamma(\alpha)(1-\alpha)}{\Gamma(\alpha)(1-\alpha)+\alpha}Q(t_k,z(t_k)) \\ &+\frac{\alpha}{\Gamma(\alpha)+\alpha(1-\Gamma(\alpha))}\sum_{v=0}^{k}\int_{t_v}^{t_{v+1}}Q(\vartheta,z(\vartheta))(t_{k+1}-\vartheta)^{\alpha-1}d\vartheta, \end{aligned} \tag{22}$$

Replacing the two-step Lagrange interpolation (9) in (22) and following the same procedures as in [29], we get

$$\begin{aligned} z(t_{k+1}) &= z(0)+\frac{(1-\alpha)\Gamma(\alpha)}{(1-\alpha)\Gamma(\alpha)+\alpha}Q(t_k,z(t_k)) \\ &+\frac{1}{(1-\alpha)(1+\alpha)\Gamma(\alpha)+\alpha}\sum_{v=0}^{k}(h^{\alpha}Q(t_v,z_v)(1+k-v)^{\alpha} \\ &(2+k-v+\alpha)-(2+k-v+2\alpha)(k-v)^{\alpha} \\ &-h^{\alpha}Q(t_{v-1},z_{v-1})(1+k-v)^{\alpha+1} \\ &-(k-v+1+\alpha)(k-v)^{\alpha}. \end{aligned} \tag{23}$$

As follows, the NS2LIM is presented:

$$\begin{aligned} z(t_{k+1}) &= z(0)+\frac{(1-\alpha)\Gamma(\alpha)}{(1-\alpha)\Gamma(\alpha)+\alpha}Q(t_k,z(t_k)) \\ &+\frac{1}{(1-\alpha)(1+\alpha)\Gamma(\alpha)+\alpha}\sum_{v=0}^{k}\phi(h)^{\alpha}Q(t_v,z_v)(1+k-v)^{\alpha} \\ &(2+k-v+\alpha)-(2+k-v+2\alpha)(k-v)^{\alpha} \\ &-\phi(h)^{\alpha}Q(t_{v-1},z_{v-1})(1+k-v)^{\alpha+1} \\ &-(k-v+1+\alpha)(k-v)^{\alpha}. \end{aligned} \tag{24}$$

This algorithm describes the solution steps of NS2LIM for the ABC model.

Algorithm 4: The ABC model approached by the NS2LIM

1- For each
•$k=0$ to n
•$v=0$ to k compute:

$$
\begin{aligned}
S(t_{k+1}) &= S(0) + \frac{(1-\alpha)\Gamma(\alpha)}{(1-\alpha)\Gamma(\alpha)+\alpha} Q(t_k, S(t_k)) \\
&+ \frac{1}{(1-\alpha)(1+\alpha)\Gamma(\alpha)+\alpha} \sum_{v=0}^{k} \phi(h)^{\alpha} Q(t_v, S_v)(1+k-v)^{\alpha} \\
&(2+k-v+\alpha) - (2+k-v+2\alpha)(k-v)^{\alpha} \\
&- \phi(h)^{\alpha} Q(t_{v-1}, S_{v-1})(1+k-v)^{\alpha+1} \\
&- (k-v+1+\alpha)(k-v)^{\alpha}, \\
E(t_{k+1}) &= E(0) + \frac{(1-\alpha)\Gamma(\alpha)}{(1-\alpha)\Gamma(\alpha)+\alpha} Q(t_k, E(t_k)) \\
&+ \frac{1}{(1-\alpha)(1+\alpha)\Gamma(\alpha)+\alpha} \sum_{v=0}^{k} \phi(h)^{\alpha} Q(t_v, E_v)(1+k-v)^{\alpha} \\
&(2+k-v+\alpha) - (2+k-v+2\alpha)(k-v)^{\alpha} \\
&- \phi(h)^{\alpha} Q(t_{v-1}, E_{v-1})(1+k-v)^{\alpha+1} \\
&- (k-v+1+\alpha)(k-v)^{\alpha}, \\
I(t_{k+1}) &= I(0) + \frac{(1-\alpha)\Gamma(\alpha)}{(1-\alpha)\Gamma(\alpha)+\alpha} Q(t_k, I(t_k)) \\
&+ \frac{1}{(1-\alpha)(1+\alpha)\Gamma(\alpha)+\alpha} \sum_{v=0}^{k} \phi(h)^{\alpha} Q(t_v, I_v)(1+k-v)^{\alpha} \\
&(2+k-v+\alpha) - (2+k-v+2\alpha)(k-v)^{\alpha} \\
&- \phi(h)^{\alpha} Q(t_{v-1}, I_{v-1})(1+k-v)^{\alpha+1} \\
&- (k-v+1+\alpha)(k-v)^{\alpha}, \\
R(t_{k+1}) &= R(0) + \frac{(1-\alpha)\Gamma(\alpha)}{(1-\alpha)\Gamma(\alpha)+\alpha} Q(t_k, R(t_k)) \\
&+ \frac{1}{(1-\alpha)(1+\alpha)\Gamma(\alpha)+\alpha} \sum_{v=0}^{k} \phi(h)^{\alpha} Q(t_v, R_v)(1+k-v)^{\alpha} \\
&(2+k-v+\alpha) - (2+k-v+2\alpha)(k-v)^{\alpha} \\
&- \phi(h)^{\alpha} Q(t_{v-1}, R_{v-1})(1+k-v)^{\alpha+1} \\
&- (k-v+1+\alpha)(k-v)^{\alpha}.
\end{aligned}
$$

End for
2- Compare the approximated results of the infected cases with the real-data.

5 Numerical results

This section includes a few numerical simulations for the model (4). Table 2 has the values of each parameter. The following starting values are used to simulate the numerical models: $S(0) = 47999990, E(0) = 3, I(0) = 7$, $R(0) = 0$, and $N(0) = 48000000$. The suggested methodology is applied to solve these mathematical equations with $h = 0.1$ and $\phi(h) = 0.3(-exp(-h)+1)$. The PC on which we utilize Matlab has a 64-bit operating system type, Core i7, Windows 10 Pro home Premium, and 8 GB of RAM.

Figure 1 shows the Caputo, Caputo-Fabrizio, and Atangana-Balenu-Caputo efficiency in predicting the infected individuals compared to the real data; we get the best results from the ABC model with $\alpha = 0.95$ with NS2LIM.

Figure 2 compares the actual data with the dynamics of the infected people under the Caputo operator utilizing various values of α. It shows a relative dimension in some cases of the chosen α values.

Figure 3 compares the actual data with the dynamics of the infected people under the Caputo-Fabrizio operator utilizing various values of α. This definition displays the least efficient approach to simulate maintained data using various α.

As seen in figure 4, the dynamics of the infected people under the Atangana-Baleanu-Caputo operator with different values of α are contrasted with actual data. It demonstrates how well this definition captures behavior that is more in keeping with the dynamics of the illness, particularly when $\alpha = 0.95$.
Figures $(5,6,7)$ illustrate how the performance of susceptible individuals, exposed individuals, and recovered individuals under ABC operator changes according to the fractional order derivatives α.
Figures $(8-11)$ show the approximate solutions of the ABC derivative considering the state variables at $\alpha = 0.95$ using NS2LIM.

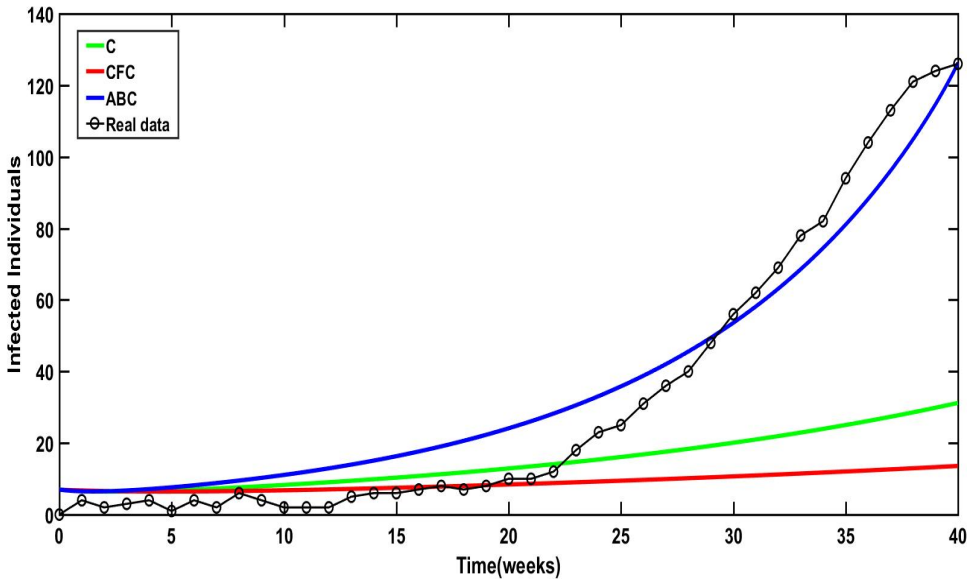

Fig. 1: Comparing real data to fractional models for infected individuals.

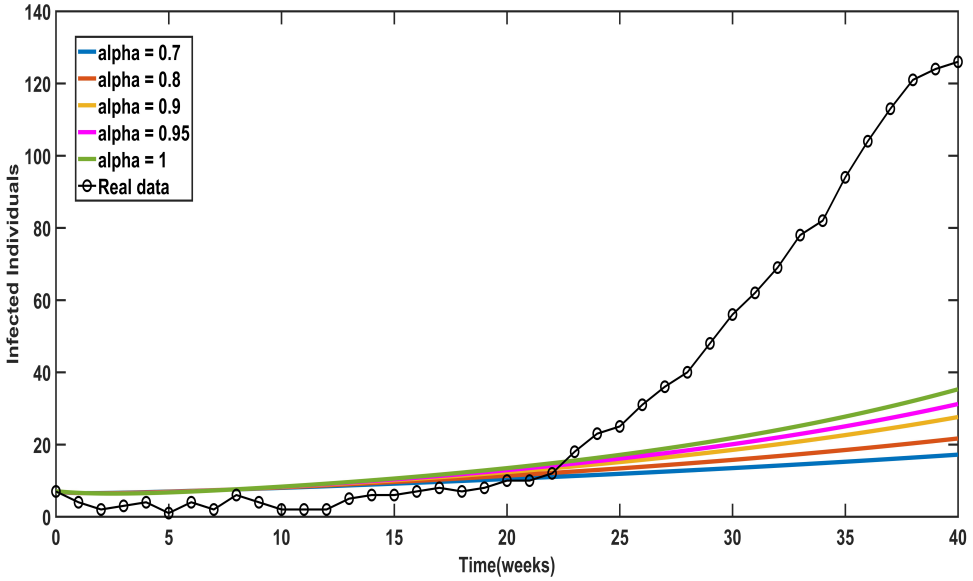

Fig. 2: Results of the Caputo operator simulation for infected persons.

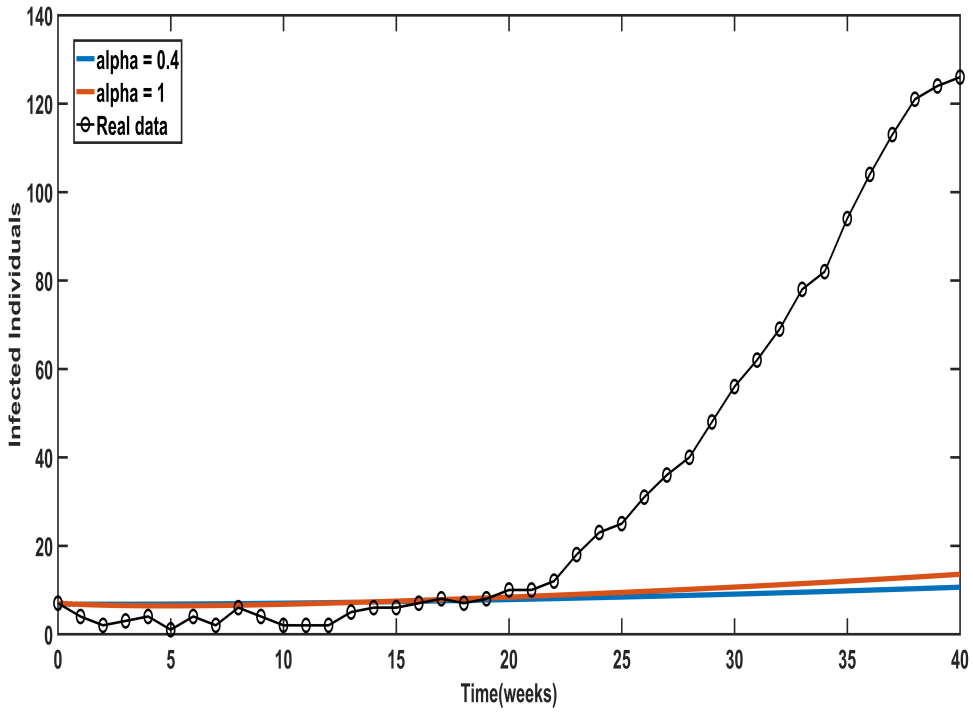

Fig. 3: Results of the CFC operator simulation for infected peoples.

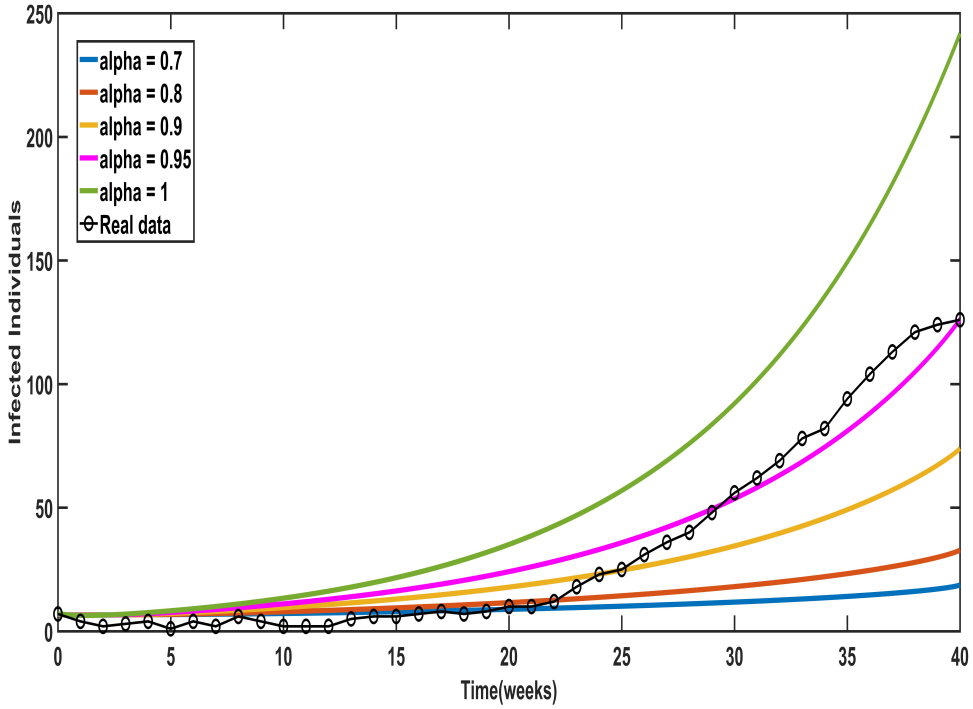

Fig. 4: Results of the ABC operator simulation for infected peoples.

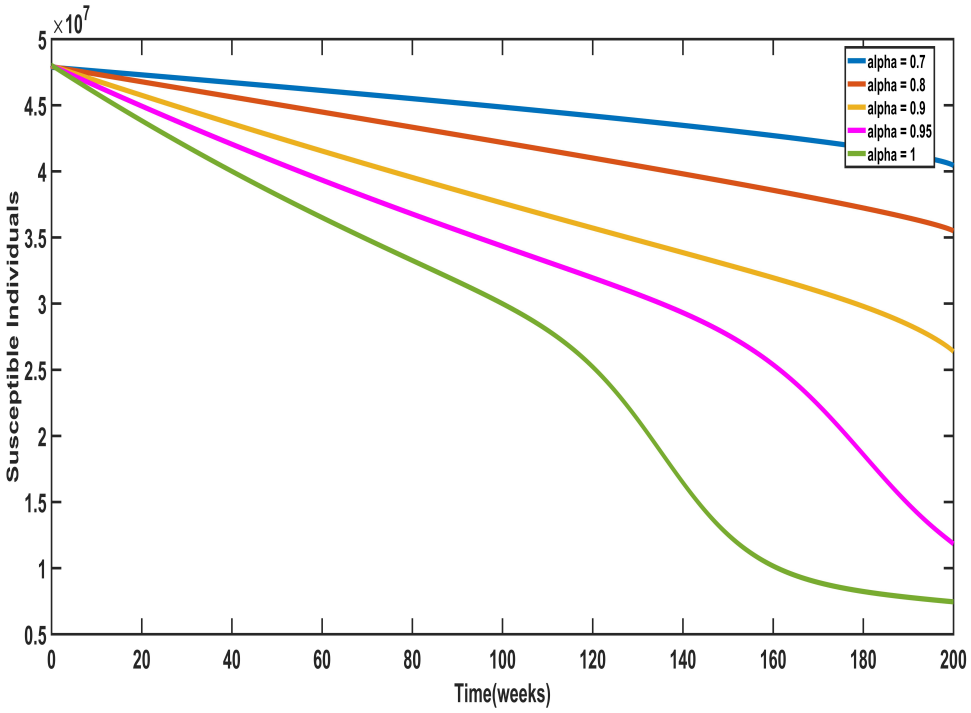

Fig. 5: The ABC operator with different α values for susceptible individuals

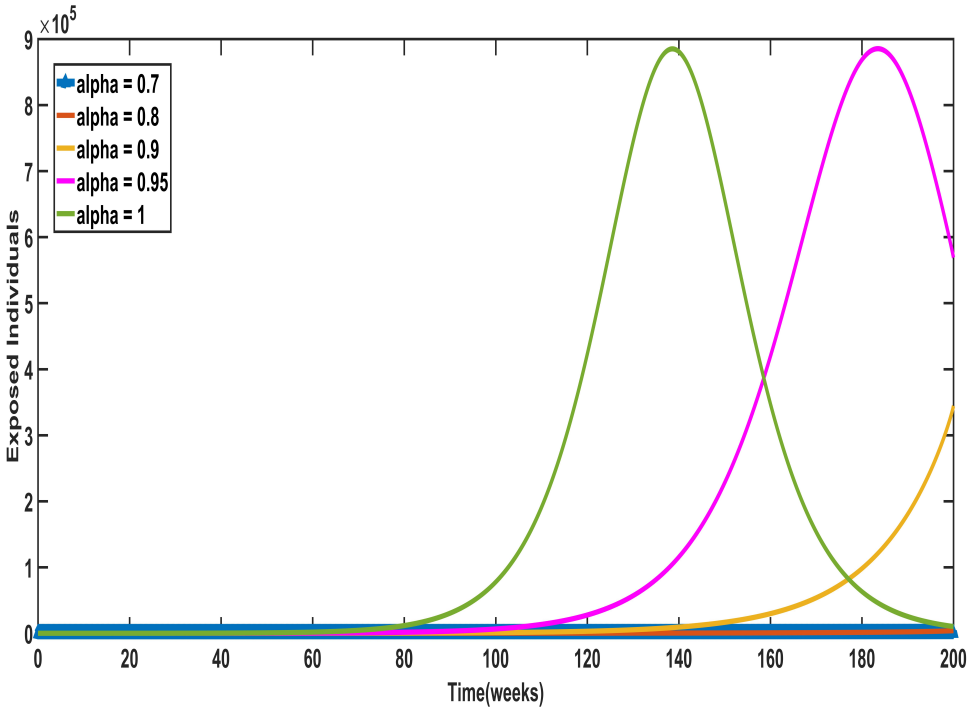

Fig. 6: The ABC operator with different α values for exposed individuals.

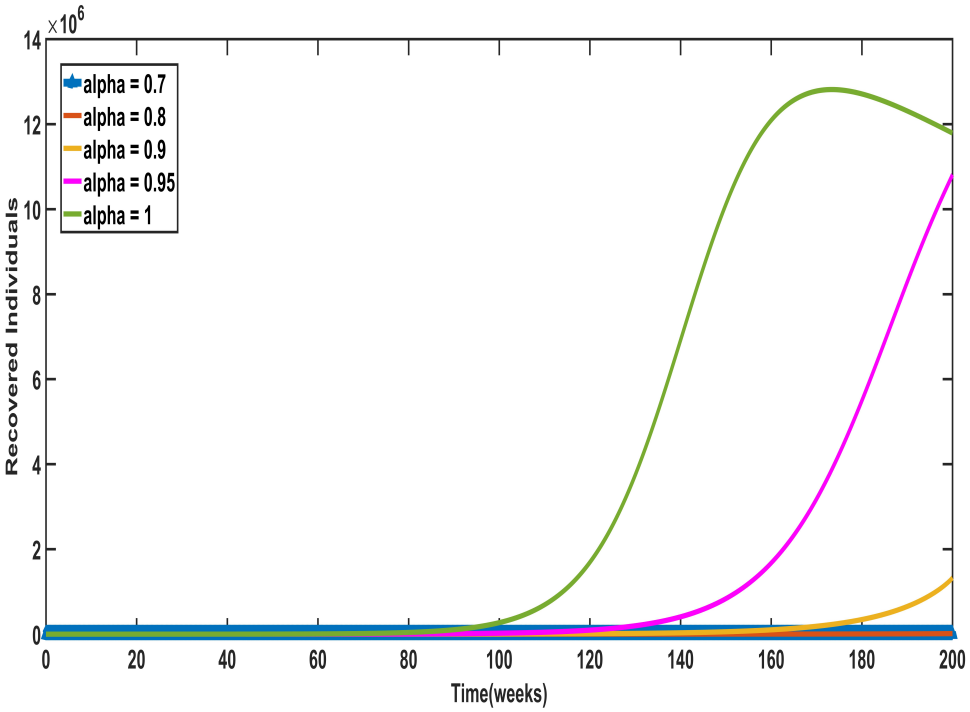

Fig. 7: The ABC operator with different α values for recovered individuals.

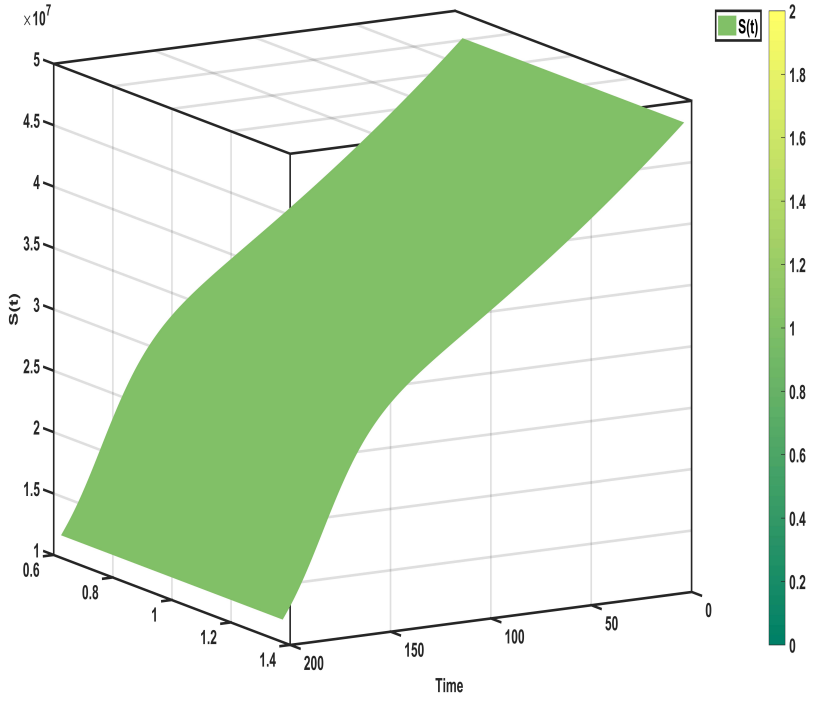

Fig. 8: Simulation state for S(t) under ABC operator with $\alpha = 0.95$, using NS2LIM.

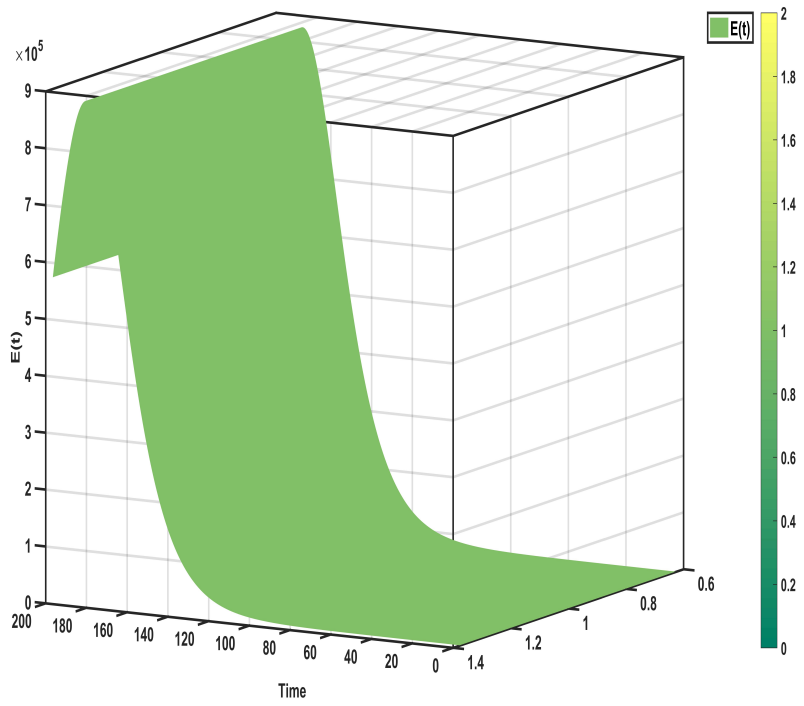

Fig. 9: Simulation state for E(t) under ABC operator with $\alpha = 0.95$, using NS2LIM.

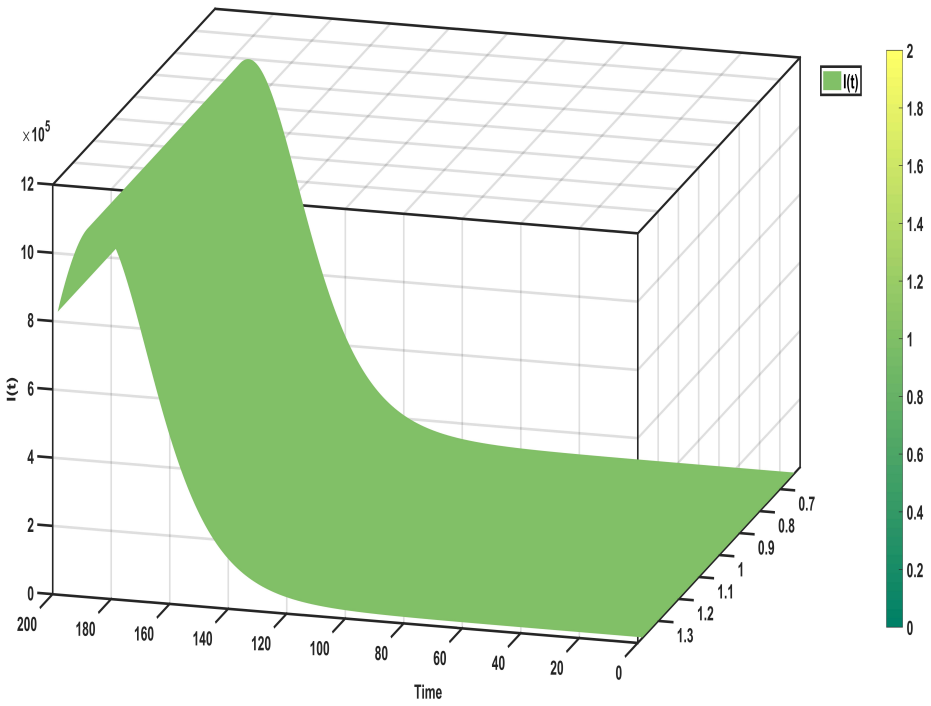

Fig. 10: Simulation state for I(t) under ABC operator with $\alpha = 0.95$, using NS2LIM.

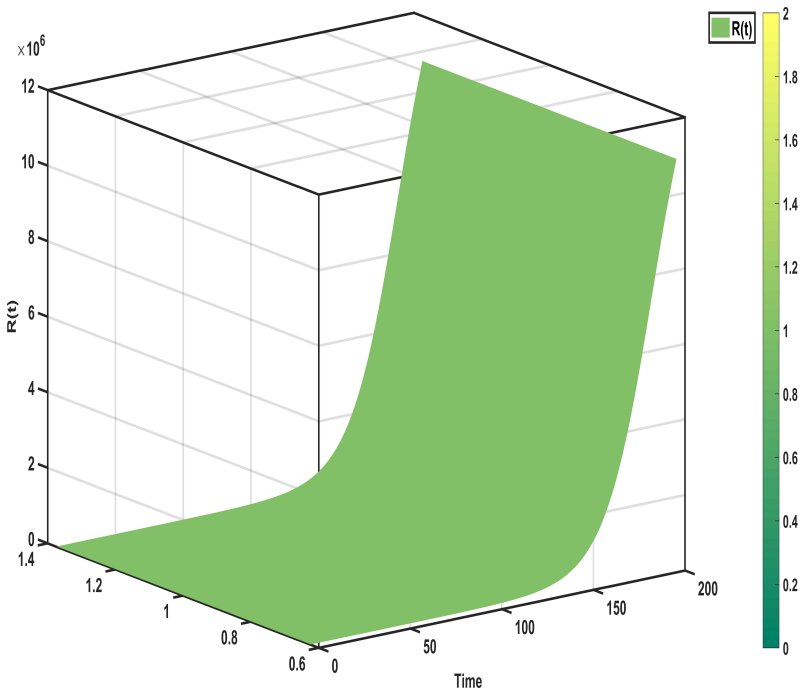

Fig. 11: Simulation state for R(t) under ABC operator with $\alpha = 0.95$, using NS2LIM.

6 Conclusion

In this paper, the epidemic model's dynamics are described using three definitions of fractional-order derivatives. The fractional-order SEIR influenza models are studied using the nonstandard two-step Lagrange interpolation method. The proposed models provide a more effective description of the SEIR model compared to existing models. We examine a Saudi Arabian influenza outbreak and feature numerical simulations to validate the precision of our findings. The NS2LIM method works simply and efficiently under C, CF, and ABC definitions, specifically the ABC definition when compared with the actual data, which gives the best results for the infected group. Future directions for this work involve developing new techniques for studying the provided model and comparing the results with those of earlier research [28].

References

[1] E.C. Hutchinson, Influenza Virus, Trends in microbiology **26**, 809–810, 9 (2018).
[2] K. Cheung, L. Poon, Biology of influenza a virus, Annals of the New York Academy of Sciences **1102(1)**, 1-25, (2007).
[3] R. Casagrandi, L. Bolzoni, S. Levin, V. Andreasen, The SIRC model and influenza A, Mathematical Biosciences **200**, 152–169, (2006).
[4] E. Mercier, P. D'Aoust, O. Thakali, et al. Municipal and neighbourhood level wastewater surveillance and subtyping of an influenza virus outbreak, Sci Rep **12**, 15777 (2022).
[5] M. Alexander, C. Bowman, S. Moghadas, R. Summers, A. Gumel, B. Sahai, A vaccination model for transmission dynamics of influenza, SIAM J. Appl. Dyn. Syst. **3**, 503–524, (2004).
[6] J. Lin, V. Andreasen, S. Levin, Dynamics of influenza a drift: the linear three strain model, Math. Biosci. **162**, 35–51, (1999).
[7] E. Murray, M. Alexander, M. Seyed, S. Moghadas, R. Gergely, W. Jianhong, A delay differential model for pandemic influenza with antiviraltreatment, Bull. J. Math. Biol. **70**, 382–397, (2008).
[8] O. Belova, O. Chuluunbaatar, M. Kapralova, N. Sweilam, The role of the bacterial mismatch repair system in SOSinduced mutagenesis: A theoretical background, J. Theor. Biol. **332**, 30–41, (2013).
[9] N. Sweilam, S. AL-Mekhlafi, A. Hassan, Numerical Treatment for Solving the fractional two-Group influenza model, Progr. Fract. Differ. **4**, 503-517, (2018).
[10] T. Cohen, M. Murray, Modeling epidemics of multidrug-resistant M. tuberculosis of heterogeneous fitness, Natur. Med. **10(10)**, 1117–1121, (2004).

[11] N. Clark, J. Lynch, Influenza: Epidemiology, clinical features, therapy, and prevention, Semin. Respir. Crit. Care Med. **32**, 373–392, (2011).
[12] R. Anderson, R. May, Infectious diseases of humans: dynamics and control, Oxford University Press: Oxford, UK, (1991).
[13] M. Sofonea, S. Cauchemez, P. Boëlle, Epidemic models: why and how to use them, Anaesth Crit Care Pain Med. **41(2)**, (2022).
[14] E. Elbasha, C. Podder, A. Gumel, Analyzing the dynamics of an SIRS vaccination model with waning natural and vaccine-induced immunity, Nonlinear Anal. Real World Appl. **12**, 2692–2705, (2011).
[15] N. Sweilam, S. AL-Mekhlafi, On the optimal control for fractional multi-strain TB model, Optim. Control Appl. Methods **37(6)**, 1355–1374, (2016).
[16] D. Baleanu, A. Jajarmi, H. Mohammadi, S. Rezapour, A new study on the mathematical modelling of human liver with Caputo–Fabrizio fractional derivative, Chaos Solitons Fractals **134**, Article ID 109705, (2020).
[17] A. Jajarmia, A. Yusuf, D. Baleanu, M. Inc, A new fractional HRSV model and its optimal control: a non-singular operator approach, Phys. A, Stat. Mech. Appl. **547**, Article ID 123860, (2020).
[18] J. Machado, Analysis and design of fractional order digital control systems, Syst. Anal. Model. Simul. **27**, 107–122, (1997).
[19] A. Salati, M. Shamsi, D. Torres, Direct transcription methods based on fractional integral approximation formulas for solving nonlinear fractional optimal control problems, Commun. Nonlinear Sci. Numer. Simul., (2018).
[20] A. Khan, G. Zaman, Optimal control strategy of SEIR endemic model with continuous age-structure in the exposed and infectious classes, Optim. Control Appl. Methods **39(5)**, 1716–1727, (2018).
[21] T. Yildiz, A fractional dynamical model for honeybee colony population, Int. J. Biomath. **11(5)**, Article ID 1850063, (2018).
[22] D. Baleanu, A. Jajarmi, On the fractional optimal control problems with a general derivative operator, Asian J. Control, (2019).
[23] N.H. Sweilam, S.M. Al-Mekhlafi, T. Assiri, A. Atanga, Optimal control for cancer treatment mathematical model using Atangana–Baleanu–Caputo fractional derivative, Adv Differ Equ **334**, (2020).
[24] N. Alsenaideh, S. Al-Mekhlafi, S. Hassan, A. Radwan, N. Sweilam, Numerical Treatment for the Distributed Order Fractional Optimal Control Coronavirus (2019-nCov) Mathematical Model, Contemp. Math. **5(4)**, 4132-6581, (2024).
[25] A. Atangana, D. Baleanu, New fractional derivatives with non-local and non-singular kernel theory and application to heat transfer model, Therm. Sci. **20(2)**, 763–769, (2016).
[26] D. Baleanu, A. Fernandez, On some new properties of fractional derivatives with Mittag-Leffler kernel, Commun. Nonlinear Sci. Numer. Simul. **18(59)**, 444–462, (2018).
[27] A. Fernandez, M. Ozarslan, D. Baleanu, On fractional calculus with general analytic kernels, Appl. Math. Comput. **354**, 248–265, (2019).
[28] M. Abdoon, R. Saadeh, M. Berir, F. EL Guma, M. ali, Analysis, modeling and simulation of a fractional-order influenza model, Alexandria Engineering Journal **74**, 231–240, (2023).
[29] J. Solís-Pérez, J. Gómez-Aguilar, A. Atangana Novel numerical method for solving variable-order fractional differential equations with power, exponential and Mittag-Leffler laws, Chaos Solitons Fractals **14**, 175–185, (2018).
[30] I. Batiha, S. Alshorm, I. Jebril, M. Hammad, A brief review about fractional calculus, Int. J. Open Probl. Compt. Math **15(4)**, (2022).
[31] N. Sweilam, Z. Mohammed, W. Abdel Kareem, Numerical approaches for solving complex order monkeypox mathematical model, Alexandria Engineering Journal **90**, 170-182, 1110-0168, (2024).
[32] Z. Ergul, I. van den Bosch, L. Gurel, Two-Step Lagrange Interpolation Method for the Multilevel Fast Multipole Algorithm, IEEE Antennas and Wireless Propagation Letters **8**, 69-71, (2009).
[33] N. Sweilam, Z. Mohammed, W. Abdel kareem, Numerical treatments for a multi-time delay complex order mathematical model of HIV/AIDS and malaria, Alexandria Engineering Journal **61**, 10263–10276, (2022).
[34] N. Sweilam, S. AL-Mekhlafi, D. Baleanu, Optimal control for a fractional tuberculosis infection model including the impact of diabetes and resistant strains, J. Adv. Res. **17**, 125–137, (2019).
[35] R. Mickens, Nonstandard finite difference models of differential equations, World Scientific, Singapore, (2005).
[36] R. Mickens, Calculation of denominator functions for nonstandard finite difference schemes for differential equations satisfying a positivity condition, Numer. Methods Partial Differ. Equ. **23**, 672–691, (2007).
[37] K. Patidar, Nonstandard finite difference methods: recent trends and further developments, J. Differ, Equ. Appl. **22(6)**, 817–849, (2016).
[38] N. Sweilam, I. Soliman, S. AL-Mekhlafi, Nonstandard finite difference method for solving the multi-strain TB model, J. Egypt. Math. Soc. **25(2)**, 129–138, (2017).
[39] N. Sweilam, S. AL-Mekhlafi, Optimal control for a nonlinear mathematical model of tumor under immune suppression: a numerical approach, Optim. Control Appl. Methods **39(5)**, 1581–1596, (2018).